Thermodynamic model of the compaction of powder materials by shock waves

Dijken, D. K.; de Hosson, J. Th. M.

Published in:
Journal of Applied Physics

DOI:
10.1063/1.355885

Publication date:
1994

Thermodynamic model of the compaction of powder materials by shock waves

D. K. Dijken and J. Th. M. De Hosson
Department of Applied Physics, Zernike Complex, University of Groningen, Nijenborgh 4, 9747 AG Groningen, The Netherlands

(Received 28 April 1993; accepted for publication 23 September 1993)

For powder materials a model is proposed to predict the mean temperature behind the shock wave, the ratio between the increase of thermal energy and increase of total internal energy, as well as the mean final temperature after release of adiabatic pressure. Further, the change of pressure, specific volume, and the internal energy behind the shock wave are calculated together with the shock-wave velocity. All these variables are supposed to depend exclusively on flyer plate velocity, initial powder density, and initial powder temperature. The ratio between the increase of thermal energy and increase of total internal energy decreases rapidly upon decreasing initial powder density, resulting in a higher shock temperature and a lower shock pressure; therefore, a lower initial powder density results in a better bonding between the particles and fewer cracks after pressure release. Calculations are carried out for copper and agree fairly well with experiments.

I. INTRODUCTION

In the compaction of powder material by shock waves there are three principal parameters affecting its performance: These are the particle or flyer plate velocity, which is mainly determined by the detonation velocity and the amount of the explosives used, the initial specific volume of the powder to be compacted, and the initial powder temperature. Other important parameters are the particle grain size and the duration of the shock pressure, which is mainly determined by the size of the experiment. Finally, the compacted powder material, still at pressure, contains both adiabatic compressive energy and thermal energy. The adiabatic part has to be transmitted to the surrounding material (flyer plate, canning material) since otherwise extensive cracking may still occur.

Depending on the materials qualities and the demands of the compactor, the principal parameters have to be adjusted to optimum values. In order to get crack-free well-sintered material, the adjustment should be a high flyer plate velocity and highly porous material, i.e., the adiabatic compressive energy is transformed to thermal energy already during the compaction process, which results in fewer cracks after pressure release. Further, the grain size should not be too small, i.e., the thermal energy is mainly deposited in the surface. In that case the surfaces of grains become hotter and it favors the sintering process. In addition, the initial temperature should be above room temperature resulting in a higher temperature behind the shock wave, leading to a better sintering process of the material. Next, the batches should be large and thick by which the material may remain for a longer time at high pressure and at high temperature. Finally, a strong and heavy canning material should be applied since the canning material will absorb the adiabatic compressive energy during pressure release.

Since the 1960s various approaches have been followed in describing the shock-wave equation of state (EOS) of powder materials. Roughly speaking, modeling was done in two different ways: i.e., semiempirically, using quasi-static powder compaction models[1–5] and purely theoretically.[6–11] Except for Ref. 11, these theoretical models adopt the Mie–Grüneisen EOS, which relates the change in internal energy to the change in pressure at constant specific volume: $dE = VdP/\Gamma(V)$. In the following a novel model is worked out, particularly devoted to powder materials research.

II. BASIC CONCEPTS

A. Shock waves in powder materials

By performing flyer plate impact experiments on a powder material there are three principle adjustable process parameters: the flyer plate velocity u_p, the initial powder specific volume V_{00}, and the initial powder temperature T_i.

For solid material the shock-wave process is schematically depicted in Fig. 1(a). Figure 1(b) shows what happens to a powder material during shock-wave compaction. The powder is represented by separate infinite thin material plates. When the first plate collapses on the shock front it behaves exactly like a solid material. Since there is some space left between the first and the second material plate, the first plate, after being compacted, starts to expand. Its compressive energy is transformed into internal kinetic energy. Then, more plates collide leaving the first plate oscillating between the flyer plate and the second plate. This goes on until all its internal kinetic energy is transformed to random thermal energy, in principle raising the temperature. Finally the first flyer plate is "locked" in its final specific volume. For material with a higher V_{00}, behind the shock wave, more compressive energy is transformed to thermal energy. At first instance this transformation step does not take place in solid material. During pressure release the (remaining) compressive energy part may be

 0021-8979/94/75(1)/203/7/$6.00

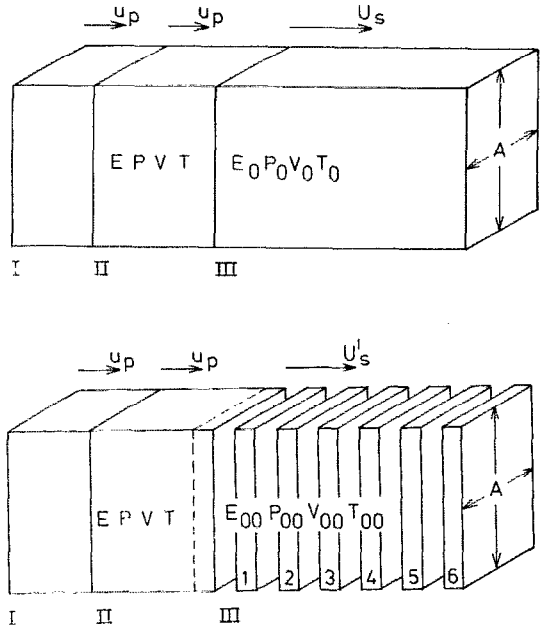

FIG. 1. (a) A rigid flyer plate impacts onto a solid or powder material. Area I is the flyerplate, area II is the compacted powder or solid material, and area III is the uncompacted powder or solid material at rest. (b) The powder is represented by separate solid plates collapsing sequentially on the shock wave front.

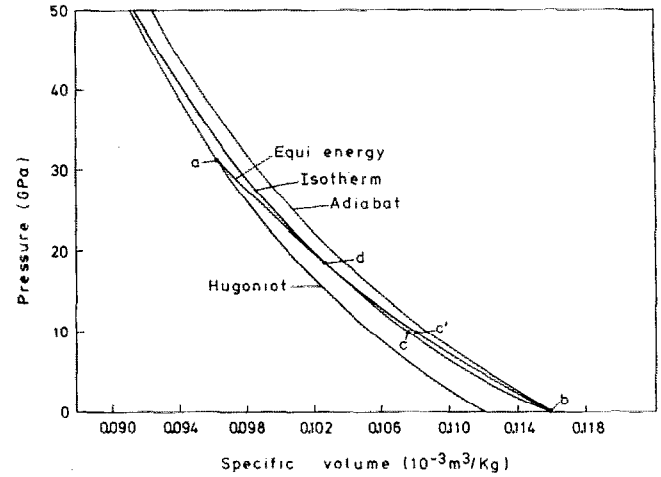

FIG. 2. Calculated Hugoniot, equienergy curve, quasistatic reversible adiabat, and isotherm.

transformed as well as transferred to the surrounding material.

The following shock-wave parameters have to be calculated as a function of these three variables: the pressure P, specific volume V, and internal energy increase $E-E_0$. The latter is the sum of adiabatic compressive energy increase E_c plus thermal energy increase E_T. Further the shock-wave velocity U_s has to be calculated as well as the temperature T and the final temperature T_f after adiabatic pressure release. All the variables are displayed in u_p vs D maps, where D is the initial density, $D=V_0/V_{00}$.

In order to derive EOS for shock-wave compacting solid and powder material, the following four assumptions are made.

(a) It is assumed that compaction of a powder at zero pressure quasistatically from V_{00} to the solid specific volume V_0 does not cost any energy, so that $E_0=E_{00}$.

(b) Behind the shock wave there are no voids present, i.e., the material is completely compacted.

(c) The increase in internal energy is equally distributed inside the compacted material. This implies that the pressure and the temperature fields are uniform. In principle this only holds for ultrafine powders since the exterior free surfaces of the grains become warmer than the interior of the grain's interior. Basic heat conductance calculations show that cooling rates can easily exceed 10^{10} °C/s. Therefore, the temperature field can be regarded as uniform.

(d) There are no volume or energy changes due to deformations or phase transformations.

B. Shock-wave equations of state for solid and powder material

For solid material the Rankine–Hugoniot shock-wave EOS for mass, momentum, and internal energy is given by,[8] writing $V_i=V_0$,

Mass:

$$VU_s=V_i(U_s-u_p), \tag{1}$$

Momentum:

$$P=\frac{U_s u_p}{V_i}, \tag{2}$$

Internal energy:

$$\delta E=E-E_0=\tfrac{1}{2}u_p^2. \tag{3}$$

Combining Eqs. (1), (2), and (3) leads to the equation

$$E-E_0=\tfrac{1}{2}P(V_i-V). \tag{4}$$

The powder material shock-wave EOS are obtained by writing $V_i=V_{00}$ and $E-E_0=E-E_{00}$, as derived in Ref. 12. Since Eq. (3) holds for both solid and powder material, the increase in internal energy is exactly the same for solid and powder material, and depends only on u_p. Therefore, the final (P,V) state point of the powder material lies on the equienergy curve, (Fig. 2). For powder of $(V_{00}\to V_0)$ or $(D\to 1)$ the (P,V) point lies close to point a. For powder of $(V_{00}\to\infty)$ or $(D\to 0)$ the (P,V) state point lies close to point b.

Recall that the work done by the flyer plate per kg of compressed material initially at rest is u_p^2 in which $\frac{1}{2}u_p^2$ per kg is converted into the internal energy of the compressed material and $\frac{1}{2}u_p^2$ per kg is converted into the kinetic energy. Here it is assumed that we are dealing with flyer plate of infinite mass and infinite stiffness (see also Ref. 2). With Eqs. (1)–(3) the P,V state points of the powder can be related to the P,V state points of the solid.

C. Solid system

The three conservation relations Eqs. (1)–(3) contain four unknown variables E, P, V, and U_s. One more relation between any two variables is necessary.

For solid and powder materials U_s can be measured at different values of u_p.[6,13] For solid material it is empirically known that the relationship between U_s and u_p is always nearly linear, i.e., $U_s=C+Su_p$, where C is approximately the zero pressure sound velocity and S is a constant. Combining Eqs. (1) and (2) with the linear relationship of U_s with u_p leads to an expression for the pressure behind the shock wave:

$$P_S=\frac{C^2(V_0-V_s)}{[V_0-S(V_0-V_s)]^2}, \tag{5}$$

which describes the solid Hugoniot which is the locus of the final shock state, but not the thermodynamic path followed by the material. The Hugoniot is an adiabat, neither an isotherm nor an isentrope. The actual thermodynamic path followed is a straight line from the initial to the final state, called the Rayleigh line.[14]

D. Equienergy curve, adiabat, and isotherm

In Fig. 2 a calculated equienergy curve, a quasistatic reversible adiabat, and an isotherm are depicted.

A material is compressed (released) adiabatically when the material is thermally isolated during the compression (release) process. The process is irreversibly adiabatic when some fraction of compressive energy is transformed to thermal energy, as in any shock compaction process. Both E_c and E_T increase with increasing pressure. An adiabatic process is called quasistatic reversible when all compressive energy can be recovered during pressure release. E_c increases with increasing pressure while E_T remains constant.

In point (b), $P=0$, $(\delta P/\delta V)_A=K_{S,P=0}$, where K_s is the adiabatic bulk modulus. With increasing pressure the temperature increases as well. The reversible adiabatic energy increases by

$$E=\int P\,dV. \tag{6}$$

In the P,V plane the equienergy curve connects all points of equal internal energy. In point b, $P=0$, $(\delta P/\delta V)_E=K_{S,P=0}$, the same as for the adiabat. With increasing pressure, the increase of E_c equals the decrease of E_T. Since the energy of equienergy curve remains constant, starting in b the pressure on the reversible adiabat is always higher.

For an isotherm in point b, $P=0$, $(\delta P/\delta V)_I=K_{T,P=0}$, where K_T is the isothermal bulk modulus. Since $K_T<K_s$ for every (P,V), starting from b the pressure on the quasistatic reversible adiabat is always higher, whereas the temperature on the adiabat is increasing. At small pressures, upon increasing the pressure, the increase in E_c is smaller than the decrease of E_T, resulting in a decrease of $E-E_0$. However, when the pressure increases approximately beyond c, the increase in E_c becomes larger than the decrease in E_T. This means (Fig. 2, starting from b between b and c, $(\delta P/\delta V)_T<(\delta P/\delta V)_E$. At point c and point c′, $(\delta P/\delta V)_{E,c}=(\delta P/\delta V)_{T,c}$. Beyond c, $(\delta P/\delta V)_T>(\delta P/\delta V)_E$. On the equienergy curve the temperature decreases from b to c′, whereas the temperature increases from c′ to a.

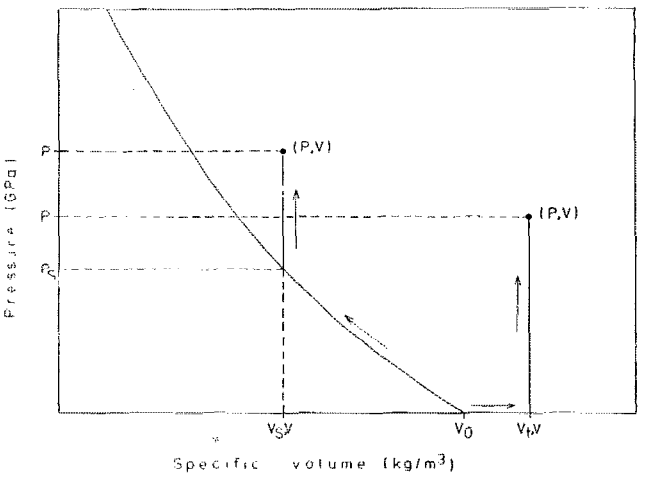

FIG. 3. Schematic representation for calculating the internal energy increase $(E-E_0)$ of (P,V) state points with respect to (P_0,V_0), in the area for $V<V_0$ and $V>V_0$.

III. CALCULATIONS

The principally adjustable process parameters in powder compaction experiments are u_p, V_{00}, and T_i. Therefore, all other shock-wave parameters have to be determined as a function of these three parameters, or $[P,V,E-E_0,U_s,T,T_f,E_T/(E-E_0)]$ as a function of u_p, V_{00}, and T_i has to be determined. At first T_i is taken equal to $T_i=T_0=293$ K.

First, $(P,V,E-E_0,U_s)$ as a function of u_p, V_{00}, and T_0 is calculated since it is independent of T, T_f, and $E_T/(E-E_0)$. The individual parameters are depicted in separate u_p vs D maps, where D is the density ratio, i.e., $D=V_0/V_{00}$. Second, $[T,T_f, E_T/(E-E_0)]$ as a function of u_p, V_{00}, and T_0 is calculated. These individual parameters are depicted as well in separate u_p vs D maps.

A. Calculation of $(P,V,E-E_0,U_s)=F(u_p,V_{00},T_0)$

For plotting the variables in u_p vs D maps, different calculation procedures are required, sometimes making a numerical calculation necessary. Therefore, $(E-E_0,u_p, U_s,V_{00})=F(P,V)$, which can be solved analytically, is calculated first, indicating the relations among the necessary basic formulas.

Suppose a powder is shock compacted to a pressure P and a volume V (Fig. 3). Its internal energy increases with respect to (P_0,V_{00}) and so (P_0,V_0), assumption a, is calculated by, for $V<V_0$,

$$E-E_0=\frac{1}{2}P_S(V_0-V)+\frac{(P-P_S)V}{\Gamma(V)}. \tag{7}$$

The first part equals the internal energy required to compact a solid from (P_0,V_0) to (P_s,V), where P_s is given by Eq. (5). The second part equals the internal energy required for heating at constant volume V from P_s to P. $\Gamma(V)$ is assumed to depend only on V, where we follow Refs. 15 and 16,

$$\Gamma(V)=\Gamma(V_0)\left(\frac{V}{V_0}\right)^q. \tag{8}$$

For Al, Cu, In, Fe, Pb, and NaCl, $\Gamma(V_0)$ and q are determined experimentally.[16] When no experimental values of $\Gamma(V_0)$ are available $\Gamma(V_0)$ can be derived from

$$\Gamma(V)=\frac{3\alpha(T)VK_S(T)}{C_P(T)}=\frac{3\alpha(T)VK_T(T)}{C_V(T)}, \tag{9}$$

where $\alpha(T)$ is the thermal-expansion coefficient, $K_T(T)$ and $K_S(T)$ are the isothermal and adiabatic bulk modulus, and $C_V(T)$ and $C_P(T)$ are the specific heats at constant volume and constant pressure (all at zero pressure). $K_S(T)$ can be calculated from $K_S(T)=C^2/V_0$ where C is the zero pressure sound velocity. When no values for q are available q can be taken to be equal to unity,[15] leading to only small errors in $\Gamma(V)$.

For $V>V_0$,

$$E-E_0=\int_{T_0}^{T_t} C_P(T)dT+\frac{PV}{\Gamma(V)}. \tag{10}$$

The first term equals the internal energy required to thermally expand at constant pressure from (T_0,V_0) to (T_t,V), where t stands for thermal expansion at zero pressure. The second term equals the internal energy required for heating at constant volume from (T_t,V) to (P,V). For many solids, over a wide temperature range, i.e., $T_0<T_t<1300$ K, $C_P(T)$ can be estimated accurately by $C_P(T)=C_P(T_0)+\gamma(T)(T_t-T_0)$. Over a wide temperature range, i.e., $T_0<T_t<1300$ K, $\alpha(T)$ can be estimated accurately by $\alpha(T)=\alpha(T_0)+\beta(T)(T-T_0)$. The volume V is related to the temperature T_t by

$$\ln\left(\frac{V}{V_0}\right)=3\alpha(T_0)(T_t-T_0)+\frac{3}{2}\beta(T)(T_t-T_0)^2. \tag{11}$$

Since the internal energy in an arbitrary (P,V) point is calculated with Eqs. (7) and (10), the particle velocity u_p, associated with these (P,V) points, is calculated from Eq. (3). By combining Eqs. (1) and (2) the shock-wave velocity is calculated. Finally, V_{00} can be derived either from Eq. (1) or Eq. (2).

Now the $(P,V,E-E_0,U_s)=F(u_p,V_{00},T_0)$ system is determined. The $(P,V,U_s)=F(u_p,D,T_0)$ maps are calculated and depicted in Figs. 4, 5, and 6, respectively. Since the $E-E_0$ equienergy in the u_p vs D maps are simply vertical straight lines, these are not depicted. Now the $(P,V,E-E_0)=F(u_p,V_{00},T_0)$ system is determined and P, V, and U_s are depicted in D vs u_p maps. In particular, for $D\rightarrow 1$ the calculated map reveals the solid system, whereas

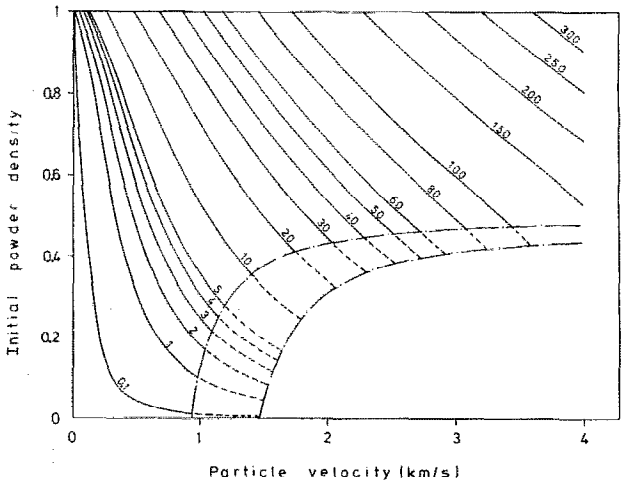

FIG. 4. Pressure (P) in GPA and internal energy ($E-E_0$). As $D\rightarrow 1$ and as $D\rightarrow 0$ the calculated map reveals the solid system and the highly porous powder system, respectively. $D=0$, $P=0$ always. $E-E_0$ is independent of D [Eq. (3)]. The model becomes less accurate due to errors in $\alpha(T)$ and $C_P(T)$ (dashed line).

for $D\rightarrow 0$ the map reveals the highly porous system. In the limit no material collides with the shock front surface and $P=0$ (Fig. 4).

B. Calculation of $[T,T_f,E_T/(E-E_0)]=F(u_p,V_{00},T_0)$

The new numerical model proposed calculates any quasistatic reversible adiabat in the P,V plane and the temperature on these adiabats. Further, the model calculates the mean temperature T, the ratio between increase of internal thermal energy, and the total internal energy increase $E_T/(E-E_0)$, both behind the shock front, and the final temperature T_f after (adiabatic) pressure release.

In principle the temperature of any point in the P,V plane can be calculated analytically, by making use of

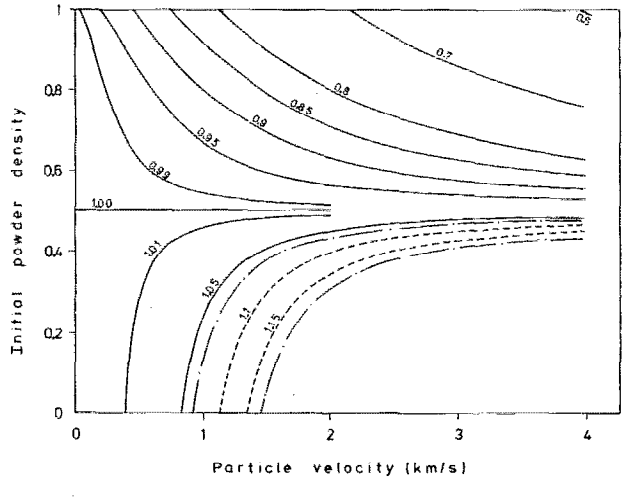

FIG. 5. Specific volume V. $D=0$, the internal energy increase is fully transformed to thermal expansion. At $D=\Gamma(V_0)/(\Gamma(V_0)+2)$, all powder material is compacted to $V=V_0$.

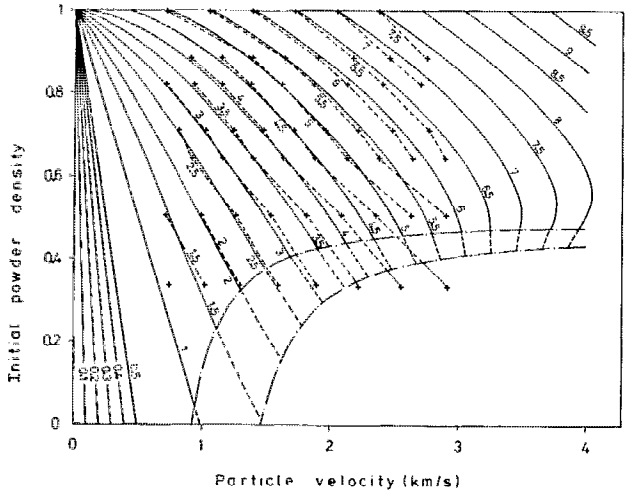

FIG. 6. Shock wave velocity U_s. The experimental points on the dashed curves are from Ref. 13. $D=0$, no material is collapsing on the shockfront surface, so $U_s=u_p$. At $u_p>\pm 3.25$ km/s at fixed u_p, different values of D can lead to the same value of U_s.

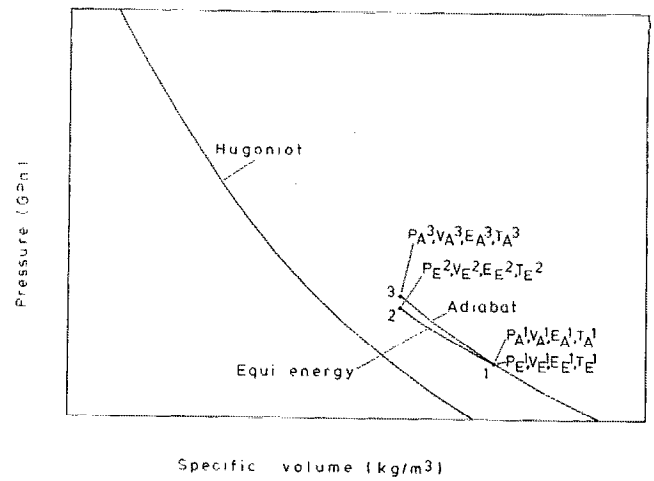

FIG. 7. Scheme for calculating the quasistatic reversible adiabat and the temperature on this adiabat. In this way the temperature behind the shock wave T is calculated in any arbitrary (P,V) point.

$$\Delta E=\frac{\Delta PV}{\Gamma(V)}=C_V(P,T)\Delta T. \tag{12}$$

and Eq. (11). Since $C_V(P,T)$, $\alpha(P,T)$, and $\beta(P,T)$ can only be obtained at $P=0$, an analytical solution is not possible. Numerically T and $E_T/(E-E_0)$ can be calculated as follows.

From basic thermodynamics it follows that the specific volume and the temperature of two points on a reversible adiabat are related by (see Ref. 14)

$$\left(\frac{\delta T}{\delta V}\right)_S=-\frac{\alpha K_S T}{C_P}=-\frac{\Gamma(V)T}{V} \tag{13}$$

or

$$\left(\frac{\delta \ln T}{\delta \ln V}\right)_S=-\Gamma(V). \tag{14}$$

Therefore, for an adiabatic compression V and T of state points 1 and 3 (Fig. 7) are related to each other by

$$\left(\frac{T_3}{T_1}\right)_s=\left(\frac{V_1}{V_3}\right)^{\Gamma(V)}. \tag{15}$$

Since $\Gamma(V)$ is a function of V, V_1 and V_3 must lie close to each other so that $\Gamma(V)$ can be approximated by $\Gamma(V)=\Gamma[(V_1+V_3)/2]$.

By compressing a material adiabatically, there is no thermal energy flux in or out the system. Therefore, increasing the adiabatic pressure results in an increase of E_C whereas E_T remains constant. In Fig. 7, E refers to state points at the equienergy curve, A refers to state points at the adiabat.

State points 1 and 2 both lie on the equienergy curve,

$$E_E^1-E_E^2=0. \tag{16}$$

The internal energy difference between state points 3 and 1 equals the surface area under the adiabat [Eq. (6)]. When $V_A^1-V_A^3$ is small, this can be written by

$$E_A^3-E_A^1=P_A^1(V_A^1-V_A^3)+\tfrac{1}{2}(P_A^3-P_A^1)(V_A^1-V_A^3). \tag{17}$$

Furthermore, the internal energy difference between state points 3 and 1 can be calculated by the Mie–Grüneisen EOS as well,

$$E_A^3-E_E^1=E_A^3-E_E^2=\frac{(P_A^3-P_E^2)V_E^2}{\Gamma^2(V)}. \tag{18}$$

Now from Eqs. (17) and (18) P_A^3 is given by

$$P_A^3=\frac{[\Gamma^2(V)P_A^1(V_A^1-V_A^3)+2P_E^2V_E^2]}{[2V_E^2-\Gamma^2(V)(V_A^1-V_A^3)]}. \tag{19}$$

By starting at $P_A^1=0$ and choosing V_A^1, T_A^1 and E_A^1 can be calculated from Eqs. (10) and (11), respectively, taking $P=0$. By choosing V_A^3, P_A^3 can be calculated from Eq. (19), E_A^3 from Eq. (7) or Eq. (10), u_p from Eq. (3), U_s from Eq. (1) together with Eq. (2), T_A^1 from Eq. (15), and finally, V_{00} from Eq. (1) or Eq. (2).

In each (P_A^3,V_A^3) point the ratio $E_T/(E-E_0)$ is calculated from the ratio $E_A^1(P=0)-E_0$ over $E_A^3(P=P_A^3)-E_0$.

By decreasing both V_A^1 and V_A^3 with a small step size of $V_A^1-V_A^3$ and repeating the above calculation procedure, the adiabat and its thermodynamic shock-wave-related variables are calculated and illustrated in D vs u_p maps. T and $E_T/(E-E_0)$ are displayed in Figs. 8 and 9. Figure 8 shows the T map. At $D=0$ the temperature behind the shock wave is roughly speaking proportional to u_p^2. Further, at $D=1$, T is relatively small compared to $D=0$ material. At $D=1$ the map shows that the adiabatic solid shock compaction process is not quasistatic reversible as $E_T/(E-E_0)$ is not equal to zero. For $D\to 0$, all compressive energy is transformed to thermal energy and $E_T/(E-E_0)=1$.

Next, the final temperature T_f, after pressure release is calculated (Fig. 10), where it is assumed that all compressive or adiabatic reversible energy E_c is transmitted to

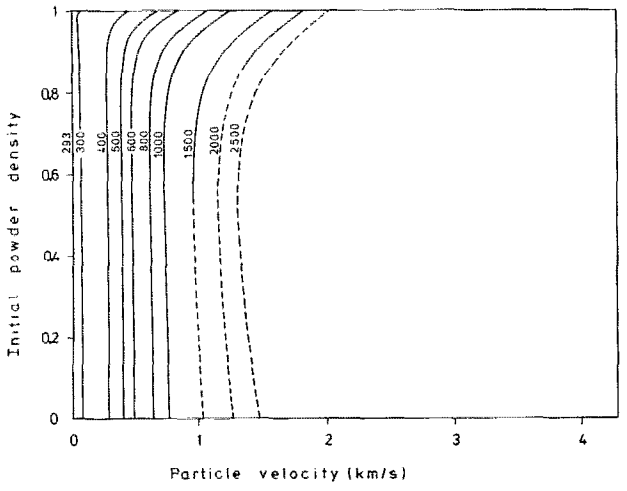

FIG. 8. Temperature T behind the shock wave. At $D=0$, T is roughly proportional with u_p^2. At fixed u_p, T can be the same for different values of D. Between $0.5 < D < 0.7$ T attains a maximum.

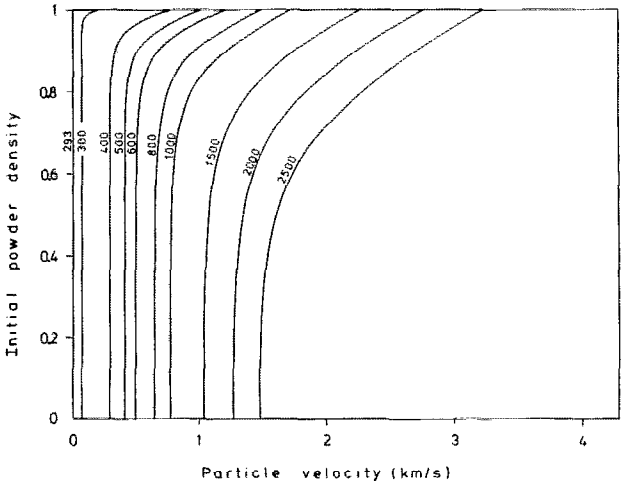

FIG. 10. Final temperature T_f after quasistatic reversible adiabatic pressure release. At $D=1$, $T_f > T$. At $D=0$, $T_f = T$, roughly proportional with u_p^2.

the surrounding material. The pressure decreases directly along the reversible adiabat to $P_A=0$. There is no oscillation of the sample at the end of the release process, therefore E_T remains constant during and after the release process. All points on the adiabat have the same T_f. If a fraction of E_c does transform to E_T the actual T_f is higher than calculated; therefore, T_f is a lower bound value.

IV. VALIDATION OF THE MODEL

U_s vs u_p relations are calculated for Cu powder material and compared with experimental data[13] and displayed in Fig. 6. Material data are listed in Table I. Calculations agree well with experiment except for initial density, flyer plate velocity combinations $D<0.64$, $u_p>2000$ m/s. The reason is the following: Because of the low density every particle oscillates many times before it finally comes at rest.

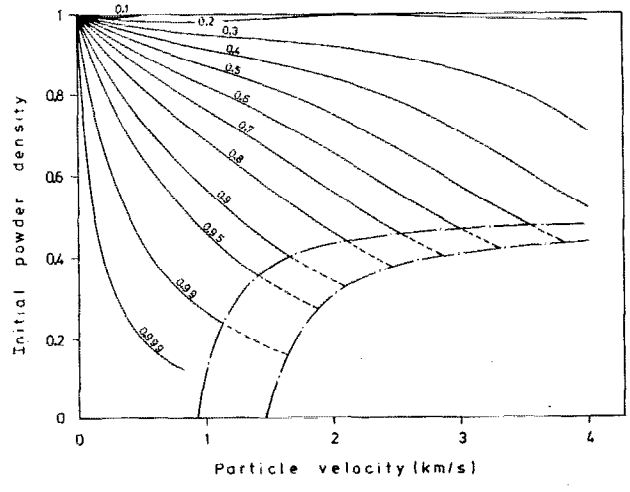

FIG. 9. Ratio between the reversible adiabatic energy E_T and the total internal energy increase $E-E_0$. At $D=1$, $E_T/(E-E_0)$ decreases until $u_p=\pm 2$ km/s after which it increases. At $D=0$, $E_T/(E-E_0)$ equals unity, all E_C has transformed to E_T.

With every collision a part of the internal energy is leaking away by microelastic shock waves through the already compacted material so that Eq. (3) changes to $\delta E < \frac{1}{2}u_p^2$. At other places in the compacted powder this energy may be consumed in the form of heat or fracture. In the calculation procedure no energy is leaking away, resulting in higher U_s values.[17]

V. CONCLUSIONS

A new EOS has been derived for shock-wave compaction of powder material to full density. The three principal adjustable shock-wave parameters are flyer plate velocity, initial powder specific volume, and initial powder temperature. As a function of these three parameters, the following shock-wave parameters were calculated: the pressure, specific volume, internal energy, ratio of thermal internal energy increase over total internal energy increase, and temperature behind the shock wave. Further, the shock-wave velocity and the temperature of the material after quasistatic adiabatic pressure release were calculated. The model is based on the fact that when a flyer plate impacts a solid or a powder material the internal energy increase

TABLE I. Experimental data of solid copper used in the calculation of shock wave EOS of powder material.

		Dimension	Ref.
C [Eq. (5)]	3910	m/s	13
S [Eq. (5)]	1.51		13
V_0	1/8930	$m^3\,kg^{-1}$	19
T_0	293	K	
q	1.3		16
$\alpha(T_0)$	16.7×10^{-6}	K^{-1}	20
$\beta(T)$	8.3×10^{-9}	K^{-2}	20
$C_p(T_0)$	383.7	$J\,kg^{-1}\,K^{-1}$	20
$\gamma(T)$	96.3×10^{-3}	$J\,kg^{-1}\,K^{-2}$	20
$C_V(T_0)$	372.7	$J\,kg^{-1}\,K^{-1}$	18
Γ	2.008		16

behind the shock wave is the same for both the solid and the powder compacted material. The model shows that: For copper at flyer plate velocities of $u_p > \pm 3500$ m/s, the model predicts that powders of different initial specific volume can have the same shock-wave velocity, for a given flyer plate velocity powders of different initial specific volume may still have the same temperature behind the shock wave, the final temperature after quasistatic adiabatic pressure release is smaller than the temperature behind the shock wave; and by increasing the initial powder temperature, the temperature behind the shock wave and the temperature after pressure release increase roughly by the same amount.

Calculations are carried out for copper. Calculations agree well with experimental values except for combinations, respectively, of initial density D and flyer plate velocity $D < 0.64$ and $u_p > 2000$ m/s.

[1] J. E. Reaugh, J. Appl. Phys. **61**, 962 (1987).
[2] K. H. Oh and P. A. Persson, J. Appl. Phys. **66**, 4736 (1989).
[3] N. W. Page and M. K. Warpenius, Powder Technol. **61**, 87 (1990).
[4] A. P. Mann, D. I. Pullin, M. N. Macrossan, and N. W. Page, J. Appl. Phys. **70**, 3281 (1991).
[5] P. Boogerd (unpublished).
[6] I. C. Skidmore and E. Morris, *Thermodynamics of Nuclear Materials* (International Atomic Agency, Vienna, 1962), p. 173.
[7] S. B. Kormer, A. I. Funtikov, V. D. Urlin, and A. N. Kolesnikova, Sov. Phys. JETP **15**, 477 (1962).
[8] Y. B. Zel'dovich and Y. P. Raizer, in *Physics of Shock Waves and High Temperature Hydrodynamic Phenomena*, edited by W. D. Hayes and R. F. Probstein (Academic, New York, 1966), Vol. 2, p. 712.
[9] T. J. Ahrens, in *Mantello e nucleo nella fisica planetaria*, edited by L. Corso, J. Coulomb, and M. Caputo (Academic, New York, 1971), p. 157.
[10] G. A. Simons and H. H. Legner, J. Appl. Phys. **53**, 943 (1982).
[11] K. H. Oh and P. A. Persson, J. Appl. Phys. **65**, 3852 (1989).
[12] D. K. Dijken and J. Th. M. De Hosson, J. Appl. Phys. (to be published).
[13] *LASL Shock Hugoniot Data*, edited by S. P. Marsh (University of California Press, Berkeley, CA, 1980).
[14] J. P. Poirier, *Introduction to the Physics of the Earth's Interior* (Cambridge University Press, Cambridge, 1991).
[15] F. D. Stacey, B. J. Brennan, and R. D. Irvine, Geophys. Surveys **4**, 189 (1981).
[16] R. Boehler, J. Ramakrishnan, and G. C. Kennedy, in *High-Pressure Science and Technology*, edited by K. D. Timmerhaus and M. S. Barber (Plenum, New York, 1979), Vol. 2, p. 119.
[17] N. N. Thadhani, Adv. Mater. Manuf. Proc. **3**, 493 (1988).
[18] *Properties of Materials at Low Temperatures*, edited by V. J. Johnson (Pergamon, Oxford, 1961).
[19] R. Kinslow, *High-Velocity Impact Phenomena* (Academic, New York, 1970).
[20] *American Institute of Physics Handbook*, edited by D. E. Gray (McGraw-Hill, New York, 1972).